JARO: 33–49 (2021)
DOI: 10.1007/s10162-020-00776-x

JARO
Journal of the Association for Research in Otolaryngology

Research Article

Effects of Kainic Acid-Induced Auditory Nerve Damage on Envelope-Following Responses in the Budgerigar (*Melopsittacus undulatus*)

John L. Wilson,[1,2,3] Kristina S. Abrams,[3] and Kenneth S. Henry[2,3,4]

[1]*University of Rochester School of Medicine & Dentistry, Rochester, NY, USA*
[2]*Department of Otolaryngology – Head & Neck Surgery, University of Rochester, Rochester, NY, USA*
[3]*Department of Neuroscience, University of Rochester, Rochester, NY, USA*
[4]*Department of Biomedical Engineering, University of Rochester, Rochester, NY, USA*

Received: 16 June 2020; Accepted: 14 October 2020; Online publication: 19 October 2020

ABSTRACT

Sensorineural hearing loss is a prevalent problem that adversely impacts quality of life by compromising interpersonal communication. While hair cell damage is readily detectable with the clinical audiogram, this traditional diagnostic tool appears inadequate to detect lost afferent connections between inner hair cells and auditory nerve (AN) fibers, known as cochlear synaptopathy. The envelope-following response (EFR) is a scalp-recorded response to amplitude modulation, a critical acoustic feature of speech. Because EFRs can have greater amplitude than wave I of the auditory brainstem response (ABR; i.e., the AN-generated component) in humans, the EFR may provide a more sensitive way to detect cochlear synaptopathy. We explored the effects of kainate-(kainic acid) induced excitotoxic AN injury on EFRs and ABRs in the budgerigar (*Melopsittacus undulatus*), a parakeet species used in studies of complex sound discrimination. Kainate reduced ABR wave I by 65–75 % across animals while leaving otoacoustic emissions unaffected or mildly enhanced, consistent with substantial and selective AN synaptic loss. Compared to wave I loss, EFRs showed similar or greater percent reduction following kainate for amplitude-modulation frequencies from 380 to 940 Hz and slightly less reduction from 80 to 120 Hz. In contrast, forebrain-generated middle latency responses showed no consistent change post-kainate, potentially due to elevated "central gain" in the time period following AN damage. EFR reduction in all modulation frequency ranges was highly correlated with wave I reduction, though within-animal effect sizes were greater for higher modulation frequencies. These results suggest that even low-frequency EFRs generated primarily by central auditory nuclei might provide a useful noninvasive tool for detecting synaptic injury clinically.

Keywords: auditory brainstem response, cochlear synaptopathy, group delay, hidden hearing loss, middle latency response, sinusoidal amplitude modulation

Correspondence to: Kenneth S. Henry · Department of Biomedical Engineering · University of Rochester · Rochester, NY, USA. email: kenneth_henry@urmc.rochester.edu

INTRODUCTION

Sensorineural hearing loss is a prevalent medical problem that can interfere with occupational functioning and adversely affect quality of life (Lin et al. 2011). While hair cell damage is readily apparent from a clinical audiogram, detection of neuronal loss remains a major clinical challenge. Progressive loss of auditory nerve (AN) afferent fibers and their synapses with inner hair cells (IHCs) occurs with normal aging and acoustic overexposure and may be due to cumulative glutamate-mediated excitotoxicity over the lifespan (Kujawa and Liberman 2009; Otte et al. 1978). Termed cochlear synaptopathy, this neuronal loss appears undetectable with an audiogram (Makary

et al. 2011; Schuknecht and Woellner 1953; Wong et al. 2019), yet has been hypothesized to cause difficulty perceiving suprathreshold speech in noise, known as "hidden hearing loss" (Bharadwaj et al. 2014; Carney 2018; Liberman and Liberman 2015; Schaette and McAlpine 2011).

Wave I of the auditory brainstem response (ABR) is the summed onset response of the AN measured at the scalp surface and provides a histologically validated measure of cochlear synaptopathy in several animal models (Bourien et al. 2014; Kujawa and Liberman 2009; Valero et al. 2017; Yuan et al. 2014). In contrast, human studies have generally failed to show consistent associations of ABR wave I amplitude with putative measures of synaptopathy in normal-hearing subjects, including self-reported prior exposure to loud sound. While Liberman et al. (2016) found lower normalized wave I amplitudes in individuals identified as at higher risk of cochlear synaptopathy, several other studies found no relationship between similar measures (Prendergast et al. 2017; Yeend et al. 2017). Part of the difficulty may be due to the low signal-to-noise ratio of ABR wave I in humans, which rarely exceeds 0.5 μV, perhaps secondary to large head circumference and thick human calvarium (Conti et al. 1988; Harris et al. 2018).

The envelope-following response (EFR) is a scalp potential evoked by amplitude-modulated sounds that has greater amplitude than ABR wave I in humans and thus might provide a more sensitive way to detect cochlear synaptopathy (Bharadwaj et al. 2015). EFRs reflect synchronization of neural responses to amplitude modulation throughout the auditory pathway, with responses to modulation frequencies less than a few hundred hertz typically associated with midbrain/cortical generation and higher modulation frequencies evoking more peripheral activity (Dolphin and Mountain 1992; Kuwada et al. 2002; Schoonhoven et al. 2003; Zhong et al. 2014). Previous studies in mice with ouabain- or noise-induced synaptopathy suggest that changes in EFR amplitude can be more sensitive to synaptopathy than ABR wave I, especially for relatively high modulation frequencies associated with AN or brainstem generation (Parthasarathy and Kujawa 2018; Shaheen et al. 2015). On the other hand, EFRs to low modulation frequencies primarily arise more centrally and therefore provide an indirect measure of peripheral AN injury that might be reduced by synaptopathy-induced changes in "central gain" (Chambers et al. 2016).

Previous animal studies have induced cochlear synaptopathy using noise overexposure (Kujawa and Liberman 2009) and neurotoxic agents including ouabain (Parthasarathy and Kujawa 2018), carboplatin (Lobarinas et al. 2013), and kainate (kainic acid; Sun et al. 2001; Wong et al. 2019). Kainate is a glutamate analog that can produce diffuse AN damage across the cochlea in mammalian and avian species through excitotoxicity without impacting hair cell integrity (Sun et al. 2001; Zheng et al. 1996). Studies in the budgerigar (*Melopsittacus undulatus*), the animal model used in the present study, show that kainate reduces ABR wave I by up to 70 % without impacting ABR thresholds, hair cell-generated otoacoustic emissions, or behavioral tone-detection thresholds (Henry and Abrams 2018; Wong et al. 2019). The diffuse localization of neural damage combined with preservation of hair cells and audiometric thresholds render kainate an interesting chemical agent for studying the physiological impact of cochlear synaptopathy.

The present study assessed the effects of kainate-induced AN damage on EFR and ABR measurements in the budgerigar (*Melopsittacus undulatus*). Budgerigars were selected because this small parrot species has a hearing range encompassing lower frequencies critical for speech comprehension in humans and shows human-like behavioral sensitivity to many simple and complex sounds (Carney et al. 2013; Dooling and Searcy 1981; Dooling et al. 2000; Henry et al. 2016, 2017, 2020). Moreover, ABR wave I in budgerigars ranges from 25 to 45 μV at 90 dB SPL and thus provides a robust measure of post-kainate AN loss (Wong et al. 2019). EFRs were recorded across a wide modulation frequency range to compare kainate effects between responses generated primarily by peripheral (380–940 Hz) vs. central (80–120 Hz) neural activity (Dolphin and Mountain 1992; Kuwada et al. 2002).

MATERIALS AND METHODS

Animals

Four budgerigars, two of each sex and approximately 2 years of age, were studied longitudinally in the present experiment. Animals K18 and K20 were male; K22 and K25 were female. The longitudinal study design allowed estimation of kainate effects on electrophysiological measures of interest within individual animals based on repeated measurements before and after exposure. All procedures were approved by the University of Rochester's Committee on Animal Resources.

Surgical Procedures

Prior to data collection, all birds underwent an initial procedure consisting of two components: (1) affixing a head post to the skull to allow for ease in stabilizing the animal's head during subsequent cochlear infusions and recording sessions and (2) implantation of a vertex electrode pin into the parieto-occipital region

of the skull bone. This latter component facilitated standardized electrode placement for subsequent electrophysiological recordings.

Surgical procedures have been previously reported (Henry and Abrams 2018; Wong et al. 2019); key aspects are described below. Prior to initiating the procedure, animals were pre-warmed in a veterinary intensive care unit (Lyon Technologies; Chula Vista, CA, USA) and anesthetized with ketamine (5–6 mg/kg) and dexmedetomidine (0.1 mg/kg). Carprofen (1 mg/kg) was given for analgesia. Induction of anesthesia was achieved via intramuscular injections into the breast muscle and maintained throughout the procedure via a continuous anesthetic infusion pump (Razel Scientific; Fairfax, VT, USA) connected to a catheter inserted subcutaneously adjacent to the thigh muscle. The infusion rate was titrated to maintain an areflexic state while also preventing hypopnea and oversedation. Following the initial injection, animals were immediately placed onto a heated water table (Adroit Medical Systems HTP-1500; Loudon, TN, USA) to minimize cooling. Respiratory rate was monitored via output from a thermistor device placed at the animal's nares. Body temperature was monitored via a thermometer (Physitemp BAT-12; Clifton, NJ, USA) with a surface probe placed directly in contact with the skin overlying the breast muscle. An electric heating pad system with feedback regulation (CWE, Inc. TC-1000; Ardmore, PA, USA) was used to maintain body temperature between 39.5 and 42.5 °C.

Once anesthetized, vertex head feathers were trimmed and the underlying scalp was sanitized with alcohol and povidone-iodine antiseptic solution. Following subcutaneous lidocaine (0.05 mL) injection for local anesthesia, ~8 mm of scalp tissue was circumferentially resected to expose the underlying bony calvarium. An excavator was used to remove residual tissue prior to the application of 37 % phosphoric acid etchant gel (Dharma Research, Inc.; Miami, FL, USA) and drilling of three 0.5 mm holes through the parieto-occipital skull; these holes provided for the insertion of the vertex electrode pin and M0.6 stainless steel anchor screws for stabilization of the head post. The head post was a hex-shaped internally threaded aluminum bar, 1/8 in. in diameter and 3/8 in. long. Following screw and electrode placement, cure composite and primer (Kerr Italia; Scafati, Italy) were applied to cement the screws, electrode, and head post into place. Anesthetic reversal was achieved with subcutaneous atipamezole (0.5 mg/kg).

Animals underwent two separate intracochlear kainate infusion procedures following the head post procedure, one to each ear, to induce bilateral and irreversible excitotoxicity-mediated AN damage localized at the AN–IHC synapse (Sun et al. 2001). Infusion procedures were separated by 4 weeks to allow for sufficient post-operative recovery and to avoid prolonged anesthetic exposure. Key details of the kainate infusion procedure are as follows (see Henry and Abrams 2018). Thermoregulation, vital sign monitoring, and anesthetic procedures were implemented as described above, with the addition of two needle electrodes inserted to generate an electrocardiogram for perioperative heart rate monitoring. After surgical site preparation, a ~5-mm incision was made over the area of the skull overlying the crossing of the horizontal and posterior semicircular canals. The overlying muscle was separated and spread apart using fine wire hooks to expose the semicircular canals, which were generally visible through the skull. Next, a craniotomy was made in the region rostral to the posterior canal and ventral to the horizontal canal, exposing the middle-ear space and basal prominence of the cochlea (Konishi 1964). After adequate exposure and hemostasis were achieved, a 150-µm cochleostomy was conducted by lowering a drill bit into the surgical field and applying gentle rotating hand pressure to the base of the cochlea until perilymph emerged. Prior to kainate delivery to the cochleostomy site, an electrode placed in contact with the perilymph was used to measure cochlear compound action potentials (see Henry and Abrams 2018). Immediately preceding the infusion, subcutaneous atropine (0.01 mg/kg) was administered to counteract potential kainate-mediated increases in vagal tone and prevent instances of bradycardia and cardiac arrest (Zaaroor and Starr 1991). The electrode was retracted before delivering 2.5 µL of 2-mM kainate solution (Abcam ab 144490; Cambridge, UK; suspended in Hanks' balanced salt solution; Sigma-Aldrich H8264; St. Louis, MO, USA) through a 35-gauge needle attached to a 10-µL syringe over 90 s. A single kainate infusion generally abolished cochlear compound action potential responses to clicks and tone frequencies spanning the full range of budgerigar hearing (0.5–6 kHz; recorded after reinsertion of the electrode), though in one case (the second procedure in K25), a second infusion was required. The wound was subsequently closed with surgical adhesive (VetOne; Boise, Idaho, USA).

Electrophysiological Measures

Following initial implantation of the head post, each animal underwent four control sessions (60–90 min each) to collect electrophysiological data prior to the two intracochlear kainate infusions (one for each ear). Experimental recording sessions occurred between the two kainate infusions (one session, during which only ABRs were recorded), as well as longitudi-

nally at 1, 2, 3, 4, 6, 8, and 12 weeks post-bilateral AN damage. For each recording session, anesthetic, thermoregulation, and monitoring procedures were conducted as previously described, except that additional anesthesia was not given following the initial bolus injection of ketamine and dexmedetomidine. Following induction of anesthesia, animals were transferred to an insulated sound booth (Acoustic Systems; Austin, TX, USA) and stationed midline in the booth. Hypodermic needle electrodes (Grass F-E2, Natus Manufacturing, Gort, Co.; Galway, Ireland) were inserted into the animal's back (ground) near wing attachments and the nape of the neck (reference); a third electrode was coupled to the chronically implanted vertex electrode.

Electrophysiological recordings were conducted using a free-field loudspeaker (Polk Audio MC60; Baltimore, MD, USA) located approximately 20 cm from the animal's head in the dorsal direction (the rostral surface of the head faced downward in the stereotaxic apparatus, with the loudspeaker and animal located in the same horizontal plane). Calibration was based on the output of a 0.25-in. precision microphone (model 4938; Brüel and Kjær, Marlborough, MA, USA) placed at the normal location of the animal's head, but with the animal removed from the apparatus, in response to pure tones. Stimuli were generated in MATLAB (MathWorks; Natick, MA, USA) with a sampling rate of 50 kHz and converted to analog via a data acquisition card (National Instruments PCIe-6251; Austin, TX, USA). Level was controlled by scaling waveform in MATLAB and through up to 60 dB of computer-controlled analog attenuation (Tucker Davis Technologies; Alachua, FL, USA). Power amplification was provided by an amplifier (Crown D75; Elkhart, IN, USA). Raw electrophysiological responses were amplified 50,000× and band-pass filtered from 30 to 10,000 Hz (Grass P511 AC amplifier, Astro-Med, Inc.; West Warwick, RI, USA), digitized at a sampling rate of 50 kHz via the data acquisition card, reconstructed graphically through MATLAB, and stored securely on a computer hard drive.

EFRs were recorded in response to sinusoidally amplitude-modulated (SAM) tone stimuli generated with 100 % modulation depth as $x(t) = [1 + \cos(2\pi f_m t + \pi)] \cdot \sin(2\pi f_c t)$, where t is time and f_c and f_m are the carrier and modulation frequencies, respectively. Three distinct modulation frequency ranges (low = 80, 100, and 120 Hz; middle = 380, 400, and 420 Hz; and high = 900, 920, and 940 Hz) were presented to facilitate inferences on neural coding in different brain regions (Dolphin and Mountain 1992). Stimuli were presented with a carrier frequency of 2.83 kHz, overall level of 75 dB SPL, and alternating carrier frequency polarity; 150 repetitions were presented for each polarity, with 130 ms of silence between successive stimuli. Each stimulus was 300 ms in duration with 10-ms cosine-squared onset and offset ramps. All stimuli contained an integer number of cycles of the modulation frequency. ABRs were recorded in response to click (100-μs duration) stimuli presented with alternating polarity at varying levels (35–90 dB peak equivalent (p.e.) SPL), with two records per level based on 100–200 click repetitions each.

Distortion product otoacoustic emissions (DPOAEs) were obtained from each ear using a closed-field system (ER10-B+ low-noise microphone with 40 dB of gain and ER2 earphones; Etymotic, Elk Grove Village, IL, USA) driven by a stereo headphone buffer (HB7; Tucker Davis Technologies) to test hair cell function before and after the two kainate infusions. In each animal, DPOAEs were recorded using a swept-tone paradigm (Long et al. 2008) once prior to the first kainate infusion and once at 8 or 12 weeks following the second kainate infusion. The DPOAE stimulus was the combination of two primary tones with linearly increasing frequencies f_1 and f_2. Primary tones were presented from separate earphones at equal sound level. f_1 swept from 0.5–6 kHz over 2 s and the ratio of f_2/f_1 was 1.25. The sound level of the primary tones ranged from 45 to 70 dB SPL in 5 dB increments (six stimuli total). Each stimulus had a cosine-squared onset and offset ramp time of 25 ms and 350 ms of silence between successive stimuli. Twenty repetitions were averaged to calculate the DPOAE level at $2f_1 - f_2$ using a least-squares fitting method implemented in MATLAB (Long et al. 2008; Wong et al. 2019); the noise floor was estimated by applying the least-squares fitting method to a null response calculated as the difference between average responses to even- and odd- numbered stimulus presentations.

Data Analysis

Primary pre- and post-kainate measures of interest included EFR amplitude and phase, middle latency response (MLR) amplitude, ABR wave I amplitude, ABR threshold, and DPOAE level. EFR amplitude and phase in response to SAM tones were calculated in the frequency domain using a discrete frequency transform at the modulation frequency of the stimulus. For modulation frequencies of 120 Hz or less, EFR amplitude was calculated as the square root of the sum of the squared FFT amplitude at the modulation frequency and at two times the modulation frequency to account for energy dispersion observed for these low modulation frequencies. EFR phase values were unwrapped as necessary and used to estimate the group delay of primary neural generators for each modulation frequency range (Bode 1945; Henry and

Lucas 2008). Group delay was calculated as the slope of the linear relationship between EFR phase and modulation frequency (in radians per Hz) divided by 2π. MLR amplitude was calculated as the peak-to-peak amplitude of the slow deflection in the SAM tone response occurring from ~15–20 ms following stimulus onset. Responses were low-pass filtered at 300 Hz (5000-point FIR) to remove the EFR prior to MLR measurement, and MLRs were not measured for modulation frequencies ≤ 120 Hz due to spectral overlap with the EFR components. ABR wave I amplitude in response to click stimuli was determined by subtracting the baseline voltage from the first major positive peak value (Brittan-Powell et al. 2002). ABR thresholds were determined as the lowest sound pressure level for which at least one ABR wave (any wave) was visible in response to two repeated presentations of the same stimulus. Thresholds were scored by an observer blinded to the animal identity and experimental condition (pre- vs. post-kainate). Finally, DPOAE level was quantified at $2f_1 - f_2$ as described above. A small proportion (< 5 %) of data was excluded from analysis due to documented technical failures, subjectively high noise levels, statistically significant outlier values (via Grubb's maximum normalized residual test) within the dataset, or thermoregulation difficulties, as EFR, ABR, and DPOAE measures appeared to be sensitive to decreases in temperature (thresholds of avian AN afferents appear stable within the normal physiological temperature range but increase by as much as 4 dB per degree decrease in body temperature below 35 °C; see Schermuly and Klinke 1985).

Statistical analyses were performed in R (version 3.6.2). Nonparametric *t* tests (Wilcoxon rank-sum test) were used to test for significant changes ($\alpha < 0.05$) in EFR amplitude, MLR amplitude, ABR wave I amplitude, and EFR group delay latency within individual animals following kainate exposure. Values of EFR, MLR, and ABR wave I amplitude were normalized on an animal-by-animal basis to facilitate data pooling across individual animals. Normalization was performed by dividing by the geometric mean value observed prior to kainate exposure in each animal. Pairwise relationships between log-transformed normalized variables (thus accounting for geometric scaling of these measures) were assessed using Pearson's product-moment correlation coefficients with 95 % confidence intervals.

Results were also analyzed at the group level using linear mixed-effects models (Bates et al. 2015) to test for a significant change following kainate exposure. Dependent variables included EFR, MLR, and ABR wave I amplitudes and DPOAE level. EFR, MLR, and ABR wave I amplitudes were log-transformed to ensure normal distribution of the model's residuals. The dependent variable for the DPOAE analysis was the median DPOAE level within the half-octave band from 1–1.41, 1.41–2, 2–2.83, 2.83–4, or 4–5.66 kHz. Subject intercepts were included as a random effect and exposure status (pre- vs. post-kainate) was a fixed effect for all analyses. An additional random effect of the test ear was nested within subjects. Other fixed effects included frequency, sound level, and two-way interactions as appropriate (all treated categorically). Nonsignificant interactions ($p > 0.05$) were dropped in order of decreasing *p* value. Degrees of freedom for *F* tests and pairwise comparisons of least-squares means were calculated based on the Satterthwaite approximation.

RESULTS

SAM Tone Responses Pre-kainate

Response waveforms following presentation of a SAM tone consisted of an oscillating phase-locked component to the stimulus modulation frequency, known as the EFR, and a slow biphasic deflection occurring from ~10–15 ms, known as the auditory MLR (Fig. 1, black traces). EFR amplitude prior to kainate exposure ranged from 0.5 to 1.5 μV and showed slightly different patterns of variation across the three modulation frequency ranges in different animals (Fig. 2a, black X symbols). MLR amplitude was greater than that of the EFR and appeared variable across animals (Fig. 2b, black X symbols; e.g., compare pre-KA MLR amplitude of 15–17 μV in animal K22 to ~5 μV in K25). In contrast to variability in MLR amplitude across animals, MLR amplitude was generally similar between the middle and high modulation frequency ranges in the same animal (Fig. 2b; note that MLRs were not analyzed for the low modulation frequency range due to spectral overlap with the EFR component of the response). Both EFRs and MLRs were reproducible across two to three repeated control sessions within individual animals, as reflected in the small error bars showing the geometric standard deviation in Fig. 2.

EFR phase was examined as a function of stimulus modulation frequency in each animal to provide insight in the primary neural generator of responses for the three modulation frequency ranges (Fig. 3, black crosses). EFR phase decreased roughly linearly with increasing modulation frequency within each modulation frequency range, consistent with a time lag or group delay of the neural response relative to the input stimulus. The calculated EFR group delay was generally longest for the low modulation frequency range (80–120 Hz), with values ranging from 4.9–11.4 ms across animals (Table 1). In contrast, group delays for EFRs to the middle (380–420 Hz) and high

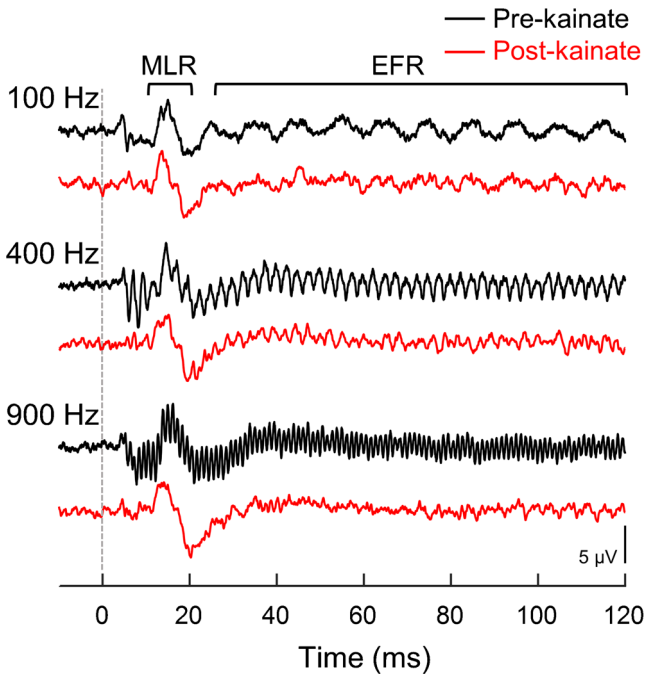

FIG. 1. Representative waveforms in response to sinusoidally amplitude-modulated (SAM) tones pre- and post-kainate. Responses from animal K18 are shown from before (black) and 8 weeks following (red) bilateral kainate exposure. The auditory middle latency response (MLR) and phase-locked envelope-following response (EFR) are denoted above the top waveform. Stimulus modulation frequency is indicated on the left. Kainate exposure reduces EFR amplitude, but not MLR amplitude

(900–940 Hz) modulation frequency ranges were shorter, ranging from 2.2–2.7 ms. These results are consistent with previous studies showing that EFRs to modulation frequencies less than a few hundred hertz originate from primarily central rather than AN- or brainstem-based neural generators (Kuwada et al. 2002; Schoonhoven et al. 2003). Note that the group delay for mid-to-high modulation frequencies was similar to the latency reported for ABR wave I in this and other species (i.e., the AN-generated component; wave I latency in budgerigars decreases from 2.6 to 1.6 ms with increasing click level from 50 to 80 dB p.e. SPL; see Henry and Abrams 2018), suggesting the EFRs to mid-to-high modulation frequencies may be dominated primarily by AN responses.

Kainate Effects on the EFR

SAM tone responses showed reduced EFR amplitude following bilateral kainate administration, a pattern evident from visual inspection of representative response waveforms in Fig. 1 (red traces). The reduction in EFR amplitude between sessions before and 1–12 weeks post-exposure was statistically significant in all animals and for every modulation frequency range tested ($p < 0.0003$; Wilcoxon rank-sum tests). EFR measurements were examined across repeated pre- and post-kainate recording sessions to assess longitudinal changes in each animal (Fig. 4a). Percent reduction of the EFR appeared greatest immediately after bilateral kainate infusions, with mild recovery plateauing at approximately 4 weeks post-exposure. Decrements in normalized EFR amplitude were most pronounced and consistent for higher modulation frequencies (≥ 380 Hz; Fig. 4a, center and right panels), for which EFRs appeared primarily generated by more peripheral (i.e., AN/brainstem) neural activity based on the group delay analysis (Table 1; Kuwada et al. 2002). Across animals, EFR amplitude was reduced by 40–60 % for modulation frequencies of 80–120 Hz (Fig. 4a, left panel), 60–80 % for modulation frequencies of 380–420 Hz (Fig. 4a, center panel), and up to 90 % for modulation frequencies of 900–940 Hz in most animals (Fig. 4a, right panel). Note, however, that kainate effects on the EFR were more variable for the highest modulation frequency range, with 80–90 % reduction observed in three animals and 60 % observed in the fourth (i.e., K25). All comparisons of EFR group delay pre- and post-kainate showed no significant change (Table 1; $p > 0.05$, Wilcoxon rank-sum tests; see Fig. 3 (red crosses) for raw EFR phase results post-kainate), suggesting no major impact of kainate on the primary site of EFR generation for all modulation frequency ranges.

Differences in geometric mean EFR amplitude between recordings made before and four or more weeks following bilateral kainate exposure (i.e., excluding data from the brief recovery period) are shown for each animal in Fig. 2a (pre-kainate: black

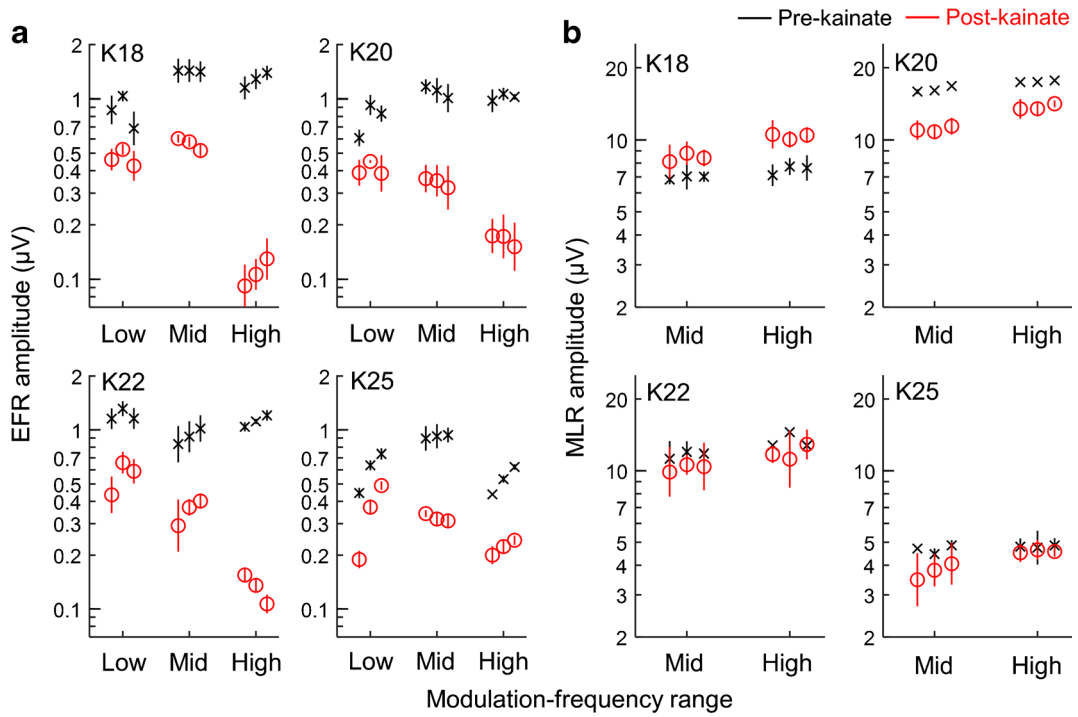

FIG. 2. EFR and MLR amplitude before and after bilateral kainate exposure. Geometric mean EFR amplitude (**a**) and MLR amplitude (**b**) of individual animals are plotted in four respective panels as a function of modulation frequency range before and four or more weeks after bilateral kainate exposure. Error bars of the pre-kainate responses indicate the geometric standard deviation across two to three repeated control sessions, except for high-frequency MLR amplitude in K20 for which repeated measurements were unavailable due to use of the line filter during the recording (which alters MLR wave shape). Post-kainate geometric means and standard deviations are based on four repeated sessions conducted from 4 to 12 weeks after bilateral kainate. Note that some error bars are nearly obscured by the symbol for the geometric mean. Neighboring data points within each modulation frequency range are separated by 20 Hz (low: 80–120 Hz; mid: 380–420 Hz; high: 900–940 Hz). MLR data are only presented for the middle and high modulation frequency ranges (see text for details). Percent reduction of the EFR is smallest in the low modulation frequency range and greatest in the high modulation frequency range. MLR amplitude is unchanged, slightly reduced, or slightly elevated following kainate exposure in different experimental animals

crosses; post-kainate: red circles). A linear mixed-effects model comparing log-transformed EFR amplitude between these two time periods showed a significant effect of kainate ($F_{1,15} = 110.36$, $p < 0.0001$) that varied across modulation frequency ranges (modulation frequency: $F_{2,15} = 9.47$, $p = 0.0022$; kainate × modulation frequency: $F_{2,15} = 9.70$, $p = 0.0020$). The reduction of log-transformed EFR amplitude was greatest for the 900–940 Hz modulation frequency range (-1.806 ± 0.191, $t_{15} = -9.48$, $p < 0.0001$; corresponding to ~84 % reduction of EFR amplitude), intermediate for the 380–420 Hz range (-1.020 ± 0.191, $t_{15} = -5.35$, $p < 0.0001$; ~64 % reduction), and lowest for modulation frequencies from 80 to 120 Hz (-0.642 ± 0.191, $t_{15} = -3.37$, $p = 0.0042$; ~47 % reduction; differences in least-squares mean log-transformed EFR amplitude ± SE).

Within-animal kainate effect sizes (d; Cohen 1988) were calculated for each animal and modulation frequency range as the mean difference in log-transformed EFR amplitude (thus accounting for geometric scaling) between repeated sessions before and 4–12 weeks after kainate exposure divided by the estimate of the pooled within-subject standard deviation (Fig. 5). Within-animal kainate effect sizes were large (i.e., absolute value greater than 2; Cohen 1988) in all cases due to consistent reduction of EFR amplitude between these two time periods, and typically increased in magnitude for higher modulation frequency ranges. Across-animal kainate effect sizes were calculated as the mean post-kainate reduction in EFR log-amplitude across animals divided by the across-subject standard deviation of the reduction. Across-animal effect sizes were 7.62, 9.97, and 2.64 for low, medium, and high modulation frequency ranges, respectively, with the smaller effect size for the high modulation frequency range due to greater variability of EFR reduction across animals (see Fig. 4a, right panel).

Kainate Effects on the MLR

In contrast to the EFR, MLRs to SAM tones, which had 10–15 ms latency consistent with a forebrain-generated response to the stimulus onset, yielded varied and relatively small changes following bilateral kainate infusion

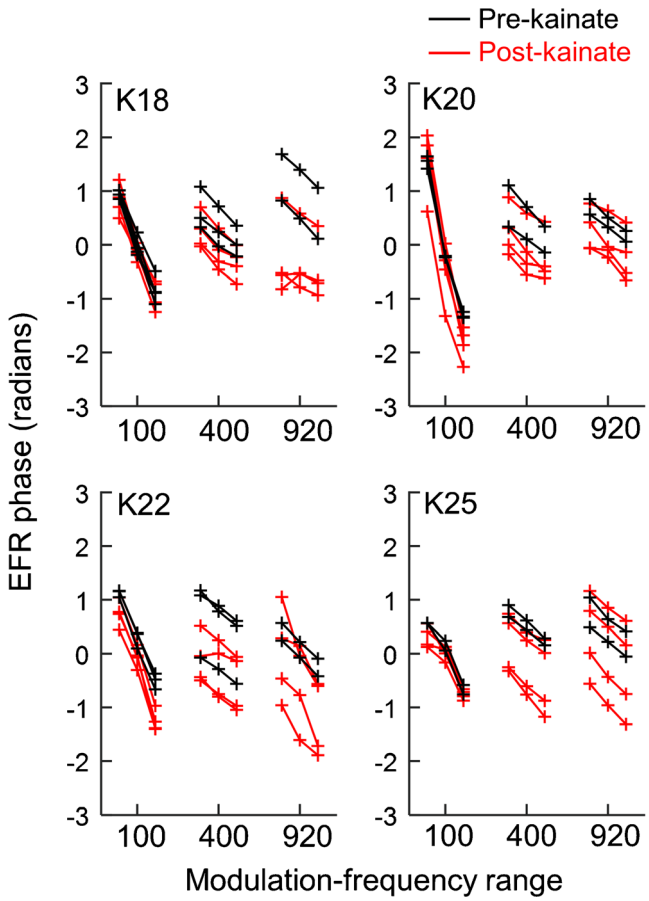

FIG. 3. EFR phase among individual animals. Raw phase measurements across repeated recording sessions conducted before and ≥ 4 weeks after bilateral kainate exposure are shown for each animal in four respective plots with neighboring data points separated by 20 Hz as in Fig. 2. Modulation frequency ranges are indicated using the middle value for each range. The slope of the relationship between EFR phase and stimulus modulation frequency is similar before and after kainate exposure, suggesting no change in the primary site of EFR generation

(see representative post-kainate response waveforms (red traces) in Fig. 1). MLR amplitude was examined across repeated recordings made pre- and post-kainate to assess longitudinal patterns of change in this response measure (Fig. 4b). In two animals, MLR amplitude decreased slightly between control sessions and sessions conducted 1–12 weeks following bilateral kainate exposure (K20: $p < 0.0001$; K25: $p = 0.005$; Wilcoxon rank-sum tests), while MLR amplitude increased (K18: $p < 0.001$; maximum enhancement occurred ~4 weeks post-exposure) or remained unchanged (K22: $p = 0.34$) for others. Overall changes in geometric mean MLR amplitude between recordings made before and 4–12 weeks post-kainate are shown in Fig. 2b (pre-kainate: black crosses; post-kainate: red circles). A linear mixed-effects model comparing log-transformed MLR amplitude between these two time periods found no group-level effects of kainate exposure or modulation frequency (kainate: $F_{1,9} = 0.98$, $p = 0.35$;

TABLE 1

Comparisons of EFR group delay, in ms (mean ± SD), pre- and post-kainate

	80–120 Hz			*380–420 Hz*			*900–940 Hz*		
	Pre-kainate	*Post-kainate*	*p*	*Pre-kainate*	*Post-kainate*	*p*	*Pre-kainate*	*Post-kainate*	*p*
K18	7.1 ± 1.0	7.2 ± 0.9	0.87	2.3 ± 0.5	2.4 ± 0.5	0.91	2.7 ± 0.2	1.8 ± 1.4	0.18
K20	11.4 ± 0.7	12.7 ± 1.4	0.15	2.5 ± 0.8	2.5 ± 0.7	0.99	2.2 ± 0.2	1.6 ± 0.6	0.24
K22	6.5 ± 0.3	7.3 ± 1.7	0.21	2.2 ± 0.4	1.7 ± 0.9	0.41	2.6	4.0 ± 1.4	0.14
K25	4.9 ± 0.5	4.3 ± 2.1	0.24	2.3 ± 0.3	2.5 ± 0.5	0.38	2.3 ± 0.3	2.6 ± 0.7	0.56

Stimulus modulation frequency range is indicated in the top row. Post-kainate data are from ≥ 1 week post-bilateral kainate exposure. There were no significant differences in group delay ($p > 0.05$, Wilcoxon rank-sum tests)

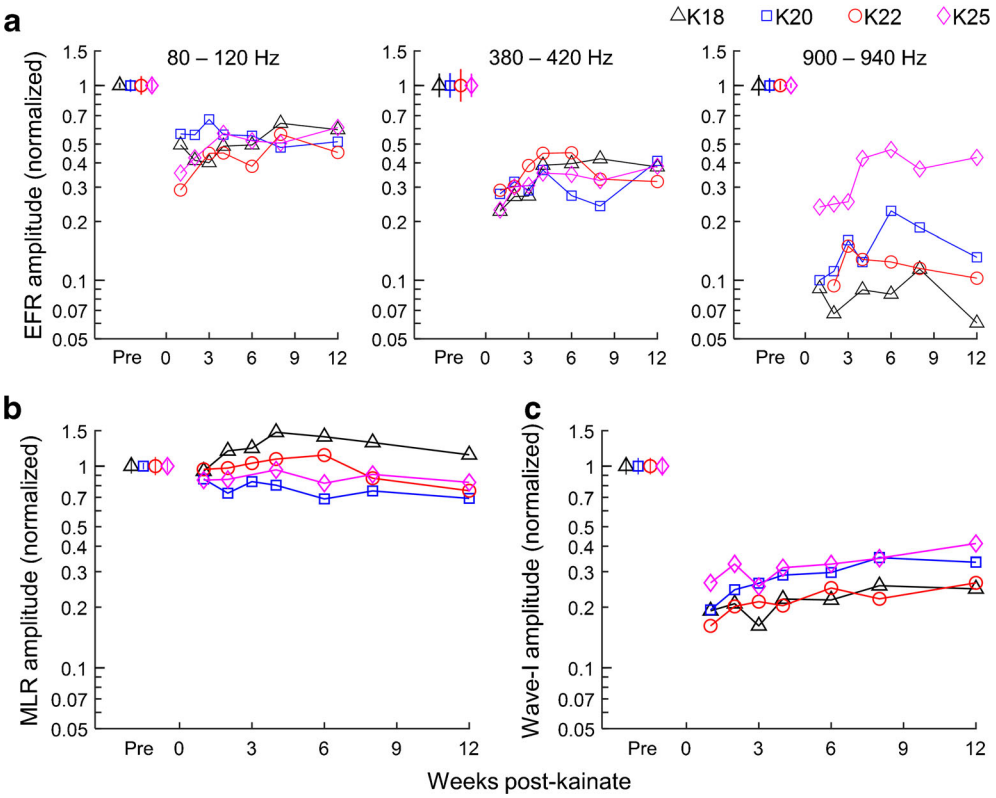

FIG. 4. Longitudinal changes in EFR amplitude (**a**), MLR amplitude (**b**), and click-evoked ABR wave I amplitude (**c**) following bilateral kainate exposure. Pre-kainate error bars indicate the geometric standard deviation across two to four repeated control sessions, and all amplitude measures were normalized by dividing by the geometric mean value observed pre-kainate in the same animal. The level of the ABR stimulus was 90 dB p.e. SPL. EFR and ABR wave I amplitudes decrease in all animals post-kainate, with greater reductions of EFR amplitude observed for higher modulation frequency ranges (indicated at top). In contrast, MLR amplitude slightly increases, slightly decreases, or remains unchanged post-kainate in different animals

modulation frequency: $F_{1,9} = 3.51$, $p = 0.094$; kainate × modulation frequency: $F_{1,9} = 0.58$, $p = 0.46$).

Within-animal kainate effect sizes on log-transformed MLR amplitude were large, but of different polarity in animals K18 and K20, and smaller in the other two animals (Fig. 5). The across-subject effect size was 0.32 (a small effect size that, if accurately estimated, would require 77 animals to detect with 80 % statistical power). These results show that while individual animals showed significant changes in MLR amplitude following kainate exposures, differences in the polarity and magnitude of the effect across animals resulted in the nonsignificant group-level effect.

Kainate Effects on ABR Wave I and ABR Thresholds

Representative ABR waveforms evoked by 35–90 dB p.e. SPL click stimuli are shown before and after bilateral kainate exposures in Fig. 6 (pre-kainate: left traces; post-kainate: right traces). Note dramatic reduction of ABR wave I post-kainate accompanied by apparent preservation of the ABR threshold (blue arrows) determined based on visual detection of later response waves. Wave I amplitude increased with increasing stimulus level and, prior to bilateral kainate, varied from 20 to 40 μV across animals at 90 dB p.e. SPL (Fig. 7, black X symbols). Unilateral administration of kainate reduced wave I by 28.3–32.2 % among the four animals (Fig. 7, magenta squares); the reduction increased to 73.6–83.8 % 1 week following the second infusion (red circles). ABR reductions were statistically significant for all animals following both unilateral ($p < 0.008$) and bilateral kainate exposure ($p < 0.0001$; Wilcoxon rank-sum tests) and were seen across stimulus levels. These findings are in general accordance with previous studies in this species using the same methodology (Henry and Abrams 2018; Wong et al. 2019), though the reason for slightly greater wave I reduction following the second kainate exposure is unknown.

Longitudinal changes in click-evoked wave I amplitude following bilateral kainate exposures are shown in Fig. 4c. Percent reduction of ABR wave I measured at 90 dB p.e. SPL was most profound immediately following bilateral kainate infusions and recovered

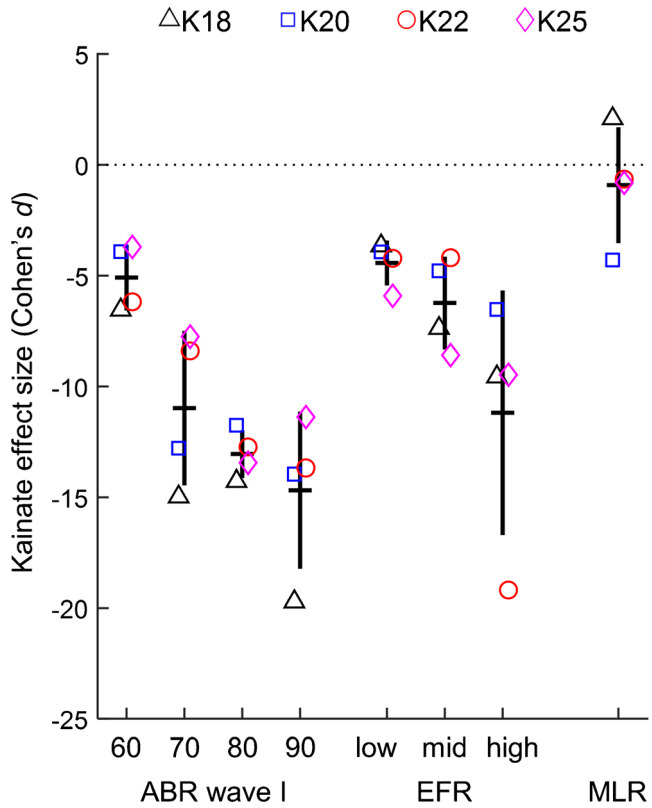

FIG. 5. Within-subject effect sizes of bilateral kainate exposure on ABR wave I amplitude, EFR amplitude, and MLR amplitude. Effect sizes were calculated in each subject as the mean difference in log-transformed response amplitude between sessions before and four or more weeks after kainate exposure, divided by the pooled within-subject standard deviation. Thick horizontal and vertical black lines indicate the mean and standard deviation of the kainate effect size across subjects, respectively. Tick labels indicate stimulus level in dB p.e. SPL for ABR wave I and the modulation frequency range for the EFR. Within-subject effect sizes are consistently large across subjects for ABR wave I and EFR amplitudes. In contrast, within-subject effects sizes on the MLR vary in polarity and magnitude across subjects

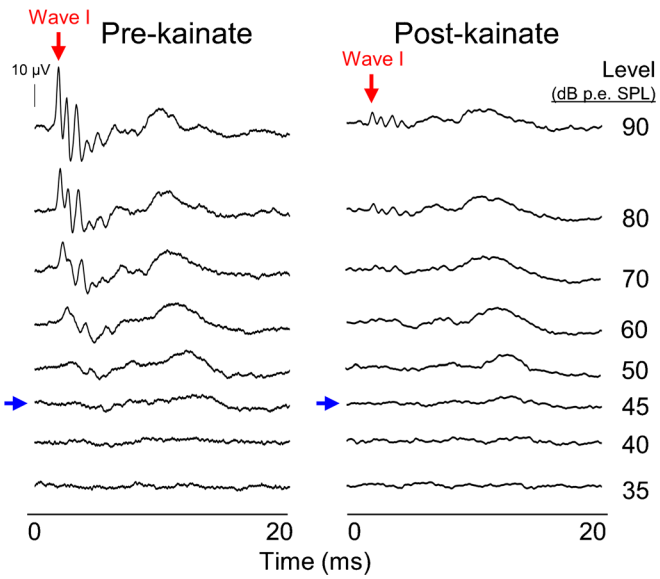

FIG. 6. Representative click-evoked ABR waveforms before and after bilateral kainate exposure. Responses are from animal K20 at stimulus levels ranging from 35 to 90 dB p.e. SPL (indicated right). Post-kainate ABRs are from 1 week following infusion of the second ear (bilateral AN damage). Stimulus threshold levels based on visual detection of any ABR wave (blue arrows; each ABR is the average of two records) appear relatively preserved despite profound reduction of ABR wave I (red arrows)

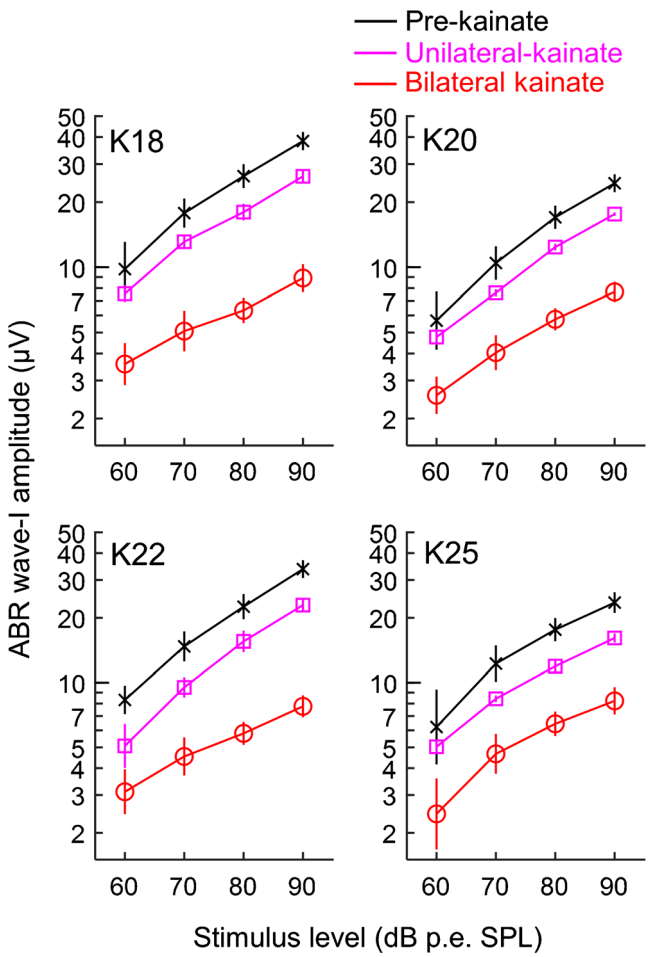

FIG. 7. ABR wave I amplitude pre- and post-kainate. Geometric mean click-evoked wave I amplitudes of individual animals are plotted in four respective panels as a function of stimulus level pre-kainate, between kainate infusions (unilateral damage), and ≥ 4 weeks after bilateral kainate exposure. Error bars indicate the geometric standard deviation across repeated measurements. Wave I reduction is significant in all animals following both unilateral and bilateral damage ($p < 0.008$ for unilateral kainate comparisons; $p < 0.0001$ for bilateral kainate comparisons; Wilcoxon rank-sum tests)

slightly (~10–15 %) over several weeks, after which ABR wave I amplitude tended to plateau and showed little further change. Overall percent reduction of ABR wave I, quantified based on all post-kainate sessions, was slightly smaller in animals K20 (68.5 % loss) and K25 (64.9 %) compared to K18 (76.6 %) and K22 (76.9 %).

Changes in geometric mean wave I amplitude between ABRs recorded before and 4–12 weeks post-kainate (i.e., after the initial recovery period) are shown in Fig. 7 (pre-kainate: black crosses; post-kainate: red circles; magenta squares show wave I amplitude in the time period between left and right ear infusions). A repeated-measures mixed-model analysis of ABR results from before and after bilateral kainate showed a substantial reduction in log-transformed ABR wave I amplitude post-kainate ($F_{1,21} = 1014.77$, $p < 0.0001$) that varied with level (level: $F_{3,21} = 203.12$, $p < 0.0001$; kainate × level: $F_{3,21} = 4.68$, $p = 0.012$). The least-squares mean change in log-transformed ABR amplitude (± SE) increased in magnitude from -0.936 ± 0.071 at 60 dB p.e. SPL (60.8 % reduction; $t_{21} = -13.20$, $p < 0.0001$) to -1.081 ± 0.071 at 70 dB p.e. SPL (66.1 % reduction; $t_{21} = -15.25$, $p < 0.0001$), -1.219 ± 0.071 at 80 dB p.e. SPL (70.5 % reduction; $t_{21} = -17.19$, $p < 0.0001$), and -1.280 ± 0.071 at 90 dB p.e. SPL (72.2 % reduction; $t_{21} = -18.06$, $p < 0.0001$).

Within-subject kainate effect sizes on log-transformed wave I amplitude were large, generally slightly exceeding values observed for EFR amplitude, and increased in magnitude with greater stimulus level (Fig. 5). The across-subject effect size was also large, with values of 8.97, 6.85, 5.98, and 6.05 for stimulus levels of 60, 70, 80, and 90 dB p.e. SPL, respectively.

ABR thresholds for click stimuli were determined as the lowest sound pressure level above which any single response wave could be visually detected in two repeated presentations of the same stimulus. ABR

thresholds typically ranged from 40 to 50 dB p.e. SPL across control sessions and showed minimal or mild elevation post-kainate (Table 2)—a pattern associated with pronounced amplitude reductions of early ABR waves (see pre- and post-kainate ABR waveforms in Fig. 6 for representative examples).

DPOAEs

DPOAE level is shown as a function of f_2 frequency in Fig. 8 at single time points before (blue traces) and 8 or 12 weeks following bilateral kainate exposure (red traces; each of the four animals was tested once before and once after kainate exposure). Individual panels show results for different primary sound levels (indicated top left), and the corresponding noise floor is shown in gray. DPOAE level prior to kainate exposures was greatest at f_2 frequencies from 1.5 to 4 kHz and increased with increasing stimulus level, as in a previous study (Wong et al. 2019). Peaks and notches were often observed in functions plotting DPOAE level as a function of frequency, particularly at low primary sound levels and high or low f_2 frequencies—a commonly observed pattern with swept-tone paradigms putatively related to the complex origin of these responses (Long et al. 2008). DPOAEs recorded following bilateral kainate infusions revealed no apparent changes compared to control recording sessions, consistent with preservation of sensory hair cells (Fig. 8, red traces). A linear mixed-effects model showed significant effects of frequency ($F_{4,440} = 261.02$, $p < 0.0001$) and sound level ($F_{5,440} = 408.70$, $p < 0.0001$; frequency × level: $F_{20,440} = 7.52$, $p < 0.0001$), due to greater DPOAE level at intermediate frequencies and higher sound levels. The effect of kainate exposure was also significant ($F_{1,440} = 21.00$, $p < 0.0001$) due to a small increase in DPOAE level following the exposure (1.48 ± 0.32 dB; $t_{440} = 4.58$, $p < 0.0001$; difference in least-squares means ± SE). DPOAE levels and the effects of kainate were similar between the two ears.

TABLE 2

ABR thresholds (dB p.e. SPL; means ± SD) before and after bilateral kainate exposure

Animal	*Pre-kainate*	*Post-kainate*	*p*
K18	43.9 ± 1.8	49.7 ± 3.9	0.029
K20	45.3 ± 1.9	45.4 ± 0.8	1
K22	41.9 ± 2.4	45.8 ± 1.7	0.11
K25	49.2 ± 2.3	54.3 ± 4.6	0.20

p values are the result of a Wilcoxon rank-sum test

Correlation Analysis

Pearson's product-moment correlation coefficients were calculated to test for relationships between EFR amplitude, ABR wave I amplitude, and MLR amplitude before and after kainate exposure (Fig. 9). Variables were normalized by the pre-exposure geometric mean to facilitate pooling of data across individual animals, and log-transformed to reflect geometric scaling of these response measures. Wave I amplitude (i.e., the AN-generated component of the ABR) was strongly correlated with SAM tone-evoked EFR amplitude for low ($r = 0.892$; 95 % CI = 0.804–0.942; $p < 0.0001$), middle ($r = 0.909$; 95 % CI = 0.831–0.951; $p < 0.0001$), and high ($r = 0.926$; 95 % CI = 0.857–962; $p < 0.0001$) modulation frequency ranges (Fig. 9). Thus, EFRs obtained in response to wide ranges of modulation frequencies were able to predict wave I reduction following kainate infusions despite putatively diverse neural origins of EFR generation. Compared to the magnitude of the reduction of ABR wave I (64.9–76.9 % reduction), the magnitude of the reduction in EFR amplitude was less for the low modulation frequency range (42.1–53.3 % reduction based on data from before and 4–12 weeks post-bilateral kainate), similar for middle modulation frequency range (60.6–68.1 % reduction), and slightly greater for the high modulation frequency range (58.1–91.3 % reduction). In contrast to EFR amplitude, MLR amplitude was uncorrelated with the amplitude of ABR wave I ($r = 0.043$; 95 % CI = –0.277–0.353; $p = 0.80$; Fig. 9).

DISCUSSION

This study examined the effects of excitotoxic AN injury from kainate on SAM tone-evoked EFRs and click-evoked ABRs in the budgerigar to test whether the EFR can provide a sensitive physiological measure of AN loss. Following bilateral intracochlear kainate administration in four animals, ABR wave I (i.e., the compound AN response; Henry and Abrams 2018) was markedly reduced as much as 80 %, and these losses were sustained longitudinally for at least 12 weeks post-exposure. EFR amplitude also decreased following kainate exposure. Reduction of EFR amplitude increased in magnitude with higher modulation frequency yet remained strongly correlated with decrements in wave I amplitude across the full range of modulation frequencies tested (80–940 Hz). In contrast, MLRs likely generated at the forebrain processing level based on their latency showed smaller and varied effects following bilateral exposure to kainate that were uncorrelated with ABR wave I loss. These results suggest that EFRs across a wide range of

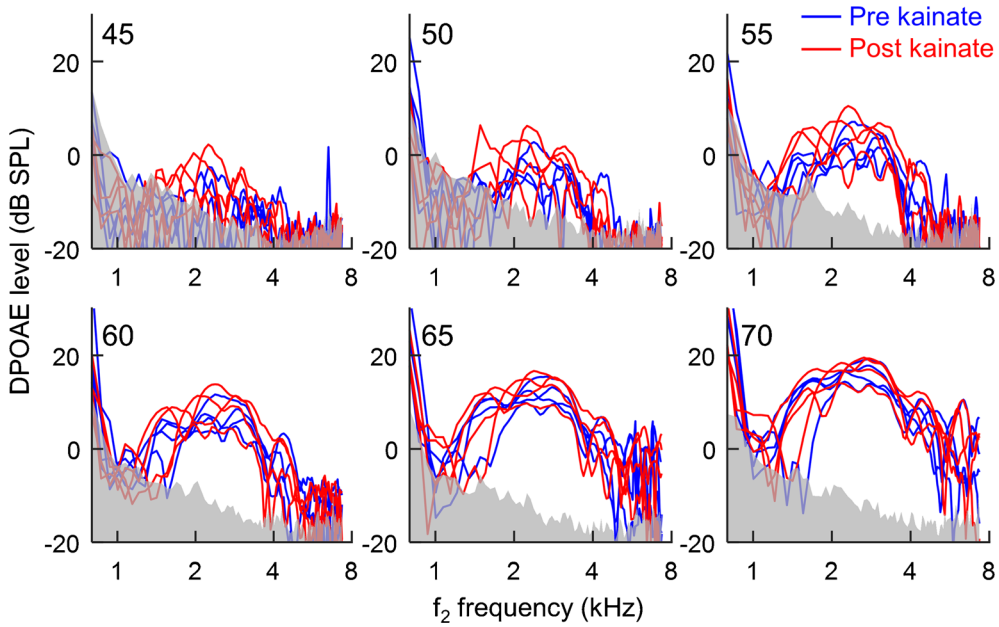

FIG. 8. Comparison of distortion product otoacoustic emissions (DPOAEs) measured before and 8 or 12 weeks following bilateral kainate exposure. DPOAE level is plotted as a function of the f_2 frequency of swept-tone stimulus presented to the right ear with the noise floor depicted in gray; left ear results are similar (data not shown). The six tested sound levels of the primary tones are indicated at the top of each panel. Kainate exposure had no apparent impact on hair cell-generated DPOAEs

modulation frequencies, including responses to low modulation frequencies putatively dominated by central neural generators, can provide a useful metric of AN excitotoxic injury.

The magnitude and durability of AN loss as measured by ABR wave I amplitude in the present study were comparable to prior work in the budgerigar, which demonstrated that amplitude losses from kainate-induced AN lesions are sustained irreversibly through at least 75 weeks post-infusion (Henry and Abrams 2018; Wong et al. 2019). Moreover, considering possible mild enhancement of DPOAE level post-kainate (Wong et al. 2019), it appears that damage from kainate originated at the level of the AN–IHC synapse rather than sensory hair cells. These inferences are congruent with a large body of previous anatomical studies in birds and mammals showing hair cell preservation following kainate-induced synaptic damage (Juiz et al. 1989; Pujol et al. 1985; Shero et al. 1998; Sun et al. 2001). Of note, measurements of AN compound action potentials immediately post-kainate revealed widespread elimination of the gross AN response across a broad frequency range (0.5–6 kHz; see Henry and Abrams 2018), suggesting that auditory afferent synaptic loss was diffuse in nature. In this light, it appears that kainate induces AN loss in a manner comparable to that which occurs in neural presbycusis (Makary et al. 2011; Mills et al. 2006; Schmiedt 2010).

Reductions in EFR amplitude following bilateral AN damage were highly correlated with reductions of ABR wave I, suggesting that like wave I, the EFR can also reflect diminished AN function following kainate excitotoxicity. Significant decrements in EFR amplitudes were observed at all studied modulation frequencies but generally increased in magnitude with increasing modulation frequency. This finding is consistent with an earlier study of EFRs in noise-overexposed mice, which found EFR amplitude reductions were most robust for higher modulation frequencies (~1 kHz in mice) and moderate stimulus levels (~70 dB SPL; Shaheen et al. 2015). EFRs to relatively high modulation frequencies may show the greatest impact from AN damage because these responses are thought to arise more primarily from the AN or auditory brainstem nuclei rather than more central generation sites (Henry and Lucas 2008; Kuwada et al. 2002; Shaheen et al. 2015); this notion is further supported by our finding that the group delay of the EFR for modulation frequencies from 380 to 940 Hz was similar to the latency of AN-generated wave I of the ABR (~2 ms in response to high-level clicks; Henry and Abrams 2018). Less clear is why EFR reduction was greater for the highest modulation frequency range than for middle modulation frequencies considering that EFRs for both ranges appeared to be primarily peripherally generated. It seems possible the kainate disproportionately damages AN afferents that encode high modulation frequencies,

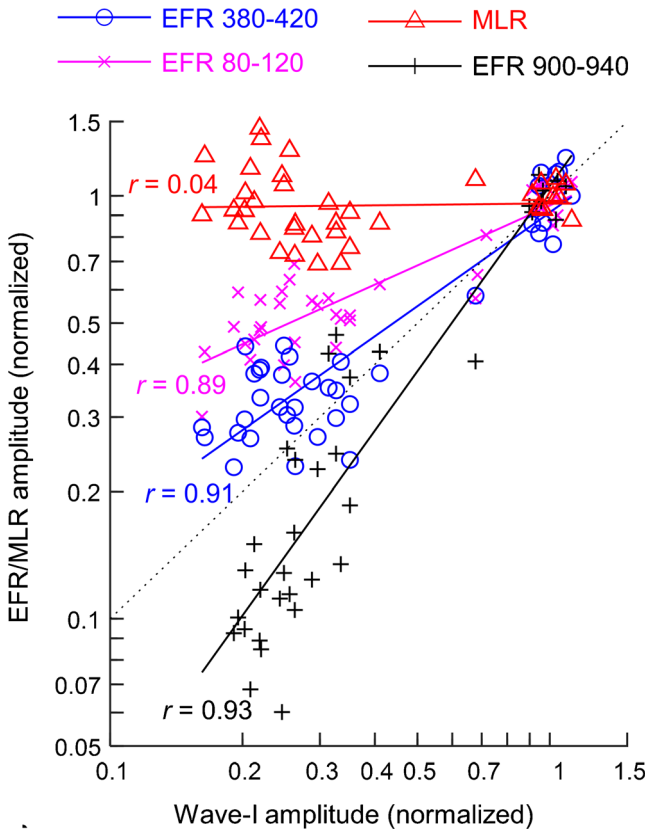

FIG. 9. Correlations of EFR and MLR amplitude with wave I amplitude of the click-evoked ABR. All amplitude measures were normalized by dividing by the geometric mean value observed pre-kainate in the same animal and are plotted on logarithmic axes to account for geometric scaling. The level of the ABR stimulus was 90 dB p.e. SPL, and each data point shows results from a single animal and test session. EFR results are plotted separately for low (80–120 Hz), middle (380–420 Hz), and high (900–940 Hz) modulation frequency ranges; MLR results are averaged across middle and high modulation frequency ranges. Colored lines indicate predicted values of a Pearson correlation; correlation coefficients, *r*, are reported to the right of each line. EFR amplitude is highly correlated with ABR wave I amplitude for all modulation frequency ranges ($p < 0.0001$; Pearson product-moment correlations), while MLR amplitude is uncorrelated with wave I amplitude ($p = 0.73$)

though no evidence exists of a fiber subpopulation specialized for high modulation frequencies and single-unit AN studies in budgerigars are currently lacking.

EFR group delay in response to modulation frequencies from 80 to 120 Hz ranged from 5 to 7 ms in most animals, suggesting generation of these responses primarily at the midbrain processing level (or perhaps a higher processing level in K20 based on ~12 ms EFR group delay) as also found in previous studies (Dolphin and Mountain 1992; Zhong et al. 2014). Despite central generation, EFR amplitude reduction in this low modulation frequency range nonetheless remained highly correlated to wave I reduction and thus appears to provide a viable avenue for detecting excitotoxic AN injury in other species such as humans for which ABR wave I amplitude is small. The relatively smaller decrements in EFR amplitude for the 80–120 Hz conditions compared to those seen for higher modulation frequencies could be due to an effect of kainate on central gain, whereby reduction of peripheral auditory input triggers a compensatory increase in the excitability of central neurons through downregulation of inhibitory signaling (Caspary et al. 2008; Chambers et al. 2016; Costalupes et al. 1984; Hickox and Liberman 2014; Salvi et al. 2017), though further study is needed to test this hypothesis.

MLRs evoked by SAM tones were differentially affected among animals, with some demonstrating modest significant increases or decreases in amplitude longitudinally and others showing no detectable change; this finding is consistent with existing literature. For instance, in comparing amplitude ratios of late (e.g., waves III and IV) to early (e.g., wave I) ABR components, Schrode et al. (2018) found generally higher ratios in noise-overexposed mice, suggestive of central compensation; however, there was considerable variation (ratios ranging from 0.5 to 2) among different animals depending on stimulus level, as well as the specific wave comparison. Nevertheless, the resilience of the SAM tone-evoked MLR in the setting of diffuse neural loss was not entirely unexpected, given that the MLR is believed to originate from

forebrain-level auditory processing centers that appear to show greater compensatory plasticity following peripheral auditory insults compared to midbrain- of brainstem-level stations (Chambers et al. 2016).

Associations of actual structural changes at the AN–IHC synapse (e.g., AN afferent fiber loss) with reductions in ABR wave I or EFR amplitudes are well characterized in other species but have not yet been studied in budgerigars. For instance, swelling of AN–IHC synapses followed by ganglion cell-body neurodegeneration have been observed in chickens and non-avian models such as mouse, rat, and guinea pig following administration of kainate (Juiz et al. 1989; Pujol et al. 1985; Shero et al. 1998) or noise overexposure (Hickox et al. 2017; Kujawa and Liberman 2009, 2015). Future studies in budgerigars need to histologically examine the neural synapse to verify the anatomical bases (e.g., synaptic swelling, reduced density of afferent fibers) of ABR and EFR changes observed in the present study.

The 1.5-dB increase in DPOAE level observed following bilateral kainate exposure was unexpected considering that previous studies in this species and others have found no significant impact of kainate on otoacoustic emissions or hair cell-generated potentials (Bledsoe et al. 1981; Henry and Abrams 2018; Sun et al. 2000, 2001; Wong et al. 2019; Zheng et al. 1996). The effect was small, however, and based on single measurements made before and after kainate exposure, raising the question of whether significant DPOAE enhancement would persist given larger samples of pre- and post-kainate measurements. Note that single measurements were made due to the extended time period required to achieve an effective seal of the DPOAE probe to ear canal. Further study is needed to determine whether mild DPOAE enhancement was anomalous (i.e., due to chance) or perhaps caused to some unknown factor influencing hair cell responses such as a post-kainate change in hair cell modulation by the efferent system.

These results can potentially help guide development of noninvasive metrics for evaluating suprathreshold hearing loss in the clinic. With considerable ABR wave I variability in humans, the EFR may provide a more robust measure of impairment at the AN– IHC synapse if it has less variance among subjects and across sessions longitudinally. Moreover, the EFR can be recorded readily in the clinical setting with transdermal electrodes. However, EFRs are traditionally recorded at lower modulation frequencies (e.g., less than 120 Hz) in humans. While low frequency (80–120 Hz) EFRs in budgerigars appeared adequate to detect AN loss in anesthetized budgerigars, future study is needed to ascertain whether this is the case in awake human subjects, which could show stronger cortically generated activity (Bramhall et al. 2019). Moreover, recent work posits that EFRs evoked by square wave-modulated tones may provide a more reliable measure of cochlear synaptopathy compared to SAM tones (Mepani et al. 2020). Prior work involving the EFR in humans shows that age-related changes in hearing may impact neural coding of temporal information (e.g., depth of amplitude modulation), but inferences are limited by a lack of histological confirmation of AN–IHC damage in humans or another means to assess synaptic viability beyond post-mortem analysis (Dimitrijevic et al. 2016; Keshishzadeh et al. 2020; Verhulst et al. 2018).

In conclusion, EFRs recorded across a wide range of modulation frequencies in anesthetized budgerigars characterized AN damage following bilateral kainate exposure in a comparable manner to AN-generated wave I of the ABR. In contrast, MLRs appeared insensitive to kainate-induced AN loss. Further study should investigate how EFR parameters directly relate to histological changes, as well as whether perceptual differences involving amplitude-modulation detection exist at specific modulation frequencies in behaviorally trained budgerigars with kainate-induced AN lesions. An enhanced understanding of how EFR changes correlate to histological changes and perceptual differences may potentially lay the foundation for translational improvements in the diagnosis and clinical management of cochlear synaptopathy and sensorineural hearing loss.

ACKNOWLEDGMENTS

Laurel Carney provided helpful comments on a previous version of the manuscript. This research was supported by a National Institute on Deafness and Other Communication Disorders grant (R00-DC013792 and R01-DC017519; P.I.: Henry) and a National Institutes of Health Ruth L. Kirschstein Individual Predoctoral National Research Service Award Fellowship (TL1 TR002000) administered by the University of Rochester Clinical and Translational Science Institute. The content of this publication is solely the responsibility of the author and does not necessarily represent the official views of the National Institutes of Health.

AUTHOR CONTRIBUTIONS

JLW and KSH designed the research, performed the experiments, analyzed the data, and wrote the manuscript. KSA performed the experiments.

COMPLIANCE WITH ETHICAL STANDARDS

Conflict of Interest The authors declare that they have no conflict of interest.

REFERENCES

BATES D, MÄCHLER M, BOLKER B, WALKER S (2015) Fitting linear mixed-effects models using lme4. J Stat Softw 67:1–48. https://doi.org/10.18637/jss.v067.i01

BHARADWAJ HM, MASUD S, MEHRAEI G, VERHULST S, SHINN-CUNNINGHAM BG (2015) Individual differences reveal correlates of hidden hearing deficits. J Neurosci 35(5):2161–2172

BHARADWAJ HM, VERHULST S, SHAHEEN L, LIBERMAN MC, SHINN-CUNNINGHAM BG (2014) Cochlear neuropathy and the coding of supra-threshold sound. Front Syst Neurosci 8:26

BLEDSOE SC, BOBBIN RP, CHIHAL DM (1981) KAINIC ACID: AN EVALUATION OF ITS ACTION ON COCHLEAR POTENTIALS. HEAR RES 4:109–120. HTTPS://DOI.ORG/10.1016/0378-5955(81)90040-X

BODE HW (1945) Network analysis and feedback amplifier design. Van Nostrand, Toronto

BOURIEN J, TANG Y, BATREL C, HUET A, LENOIR M, LADRECH S, DESMADRYL G, NOUVIAN R, PUEL JL, WANG J (2014) Contribution of auditory nerve fibers to compound action potential of the auditory nerve. J Neurophysiol 112(5):1025–1039

BRAMHALL N, BEACH EF, EPP B, LE PRELL CG ET AL (2019) The search for noise-induced cochlear synaptopathy in humans: mission impossible? Hear Res 377:88–103

BRITTAN-POWELL EF, DOOLING RJ, GLEICH O (2002) Auditory brainstem responses in adult budgerigars (*Melopsittacus undulatus*). J Acoust Soc Am 112:999–1008. https://doi.org/10.1121/1.1494807

CARNEY LH (2018) Supra-threshold hearing and fluctuation profiles: implications for sensorineural and hidden hearing loss. J Assoc Res Otolaryngol 19:331–352

CARNEY LH, KETTERER AD, ABRAMS KS, SCHWARZ DM, IDROBO F (2013) Detection thresholds for amplitude modulations of tones in budgerigar, rabbit, and human. Adv Exp Med Biol 787:391–398. https://doi.org/10.1007/978-1-4614-1590-9_43

CASPARY DM, LING L, TURNER JG, HUGHES LF (2008) Inhibitory neurotransmission, plasticity and aging in the mammalian central auditory system. J Exp Biol 211:1781–1791. https://doi.org/10.1242/jeb.013581

CHAMBERS AR, RESNIK J, YUAN Y, WHITTON JP, EDGE AS, LIBERMAN MC, POLLEY DB (2016) Central gain restores auditory processing following near-complete cochlear denervation. Neuron. 89(4):867–879

COHEN J (1988) Statistical power analysis for the behavioral sciences. Laurence Erlbaum Associates, USA

CONTI G, MODICA V, CASTRATARO A, FILENI A, COLOSIMO C JR (1988) Latency of the auditory brainstem response (ABR) and head size: evidence of the relationship by means of radiographic data. Scand Audiol Suppl 30:219–223

COSTALUPES JA, YOUNG ED, GIBSON DJ (1984) Effects of continuous noise backgrounds on rate response of auditory-nerve fibers in cat. J Neurophysiol 51(6):1326–1344

DIMITRIJEVIC A, ALSAMRI J, JOHN MS, PURCELL D, GEORGE S, ZENG F (2016) Human envelope following responses to amplitude modulation: effects of aging and modulation depth. Ear Hear 37(5):e322–e335

DOLPHIN WF, MOUNTAIN DC (1992) The envelope following response: scalp potentials elicited in the Mongolian gerbil using sinusoidally AM acoustic signals. Hear Res 58(1):70–78

DOOLING RJ, LOHR B, DENT ML (2000) Hearing in birds and reptiles. In: Dooling RJ, Fay RR, Popper AN (eds) Comparative hearing: birds and reptiles. Springer, New York, pp 308–359

DOOLING RJ, SEARCY MH (1981) Amplitude modulation thresholds for the parakeet (*Melopsittacus undulatus*). J Comp Physiol 43:383–388. https://doi.org/10.1007/BF00611177

HARRIS KC, VADEN KI, MCCLASKEY CM, DIAS JW, DUBNO JR (2018) Complementary metrics of human auditory nerve function derived from compound action potentials. J Neurophysiol 119(3):1019–1028. https://doi.org/10.1152/jn.00638.2017

HENRY KS, ABRAMS KS (2018) Persistent auditory nerve damage following kainic acid excitotoxicity in the budgerigar (*Melopsittacus undulates*). J Assoc Res Otolaryngol 19(4):435–449

HENRY KS, AMBURGEY KN, ABRAMS KS, CARNEY LH (2020) Identifying cues for tone-in-noise detection using decision variable correlation in the budgerigar (*Melopsittacus undulatus*). J Acoust Soc Am 147:984–997

HENRY KS, AMBURGEY KN, ABRAMS KS, IDROBO F, CARNEY LH (2017) Formant-frequency discrimination of synthesized vowels in budgerigars (*Melopsittacus undulatus*) and humans. J Acoust Soc Am 142:2073–2083. https://doi.org/10.1121/1.5006912

HENRY KS, LUCAS JR (2008) Coevolution of auditory sensitivity and temporal resolution with acoustic signal space in three songbirds. Anim Behav 76:1659–1671

HENRY KS, NEILANS EG, ABRAMS KS, IDROBO F, CARNEY LH (2016) Neural correlates of behavioral amplitude modulation sensitivity in the budgerigar midbrain. J Neurophysiol 115(4):1905–1916

HICKOX AE, LARSEN E, HEINZ MG, SHINOBU L, WHITTON JP (2017) Translational issues in cochlear synaptopathy. Hear Res 349:164–171. https://doi.org/10.1016/j.heares.2016.12.010

HICKOX AE, LIBERMAN MC (2014) Is noise-induced cochlear neuropathy key to the generation of hyperacusis or tinnitus? J Neurophysiol 111:552–564. https://doi.org/10.1152/jn.00184.2013

JUIZ JM, RUEDA J, MERCHÁN JA, SALA ML (1989) The effects of kainic acid on the cochlear ganglion of the rat. Hear Res 40:65–74. https://doi.org/10.1016/0378-5955(89)90100-7

KESHISHZADEH S, GARRETT M, VASILKOV V, VERHULST S (2020) The derived-band envelope following response and its sensitivity to sensorineural hearing deficits. Hear Res 392:107979. https://doi.org/10.1016/j.heares.2020.107979

KONISHI M (1964) Effects of deafening on song development in two species of juncos. Condor 66:85–102

KUJAWA SG, LIBERMAN MC (2009) Adding insult to injury: cochlear nerve degeneration after "temporary" noise-induced hearing loss. J Neurosci 29:14077–14085. https://doi.org/10.1523/JNEUROSCI.2845-09.2009

KUJAWA SG, LIBERMAN MC (2015) Synaptopathy in the noise-exposed and aging cochlea: primary neural degeneration in acquired sensorineural hearing loss. Hear Res 330:191–199

KUWADA S, ANDERSON JS, BATRA R, FITZPATRICK DC, TEISSIER N, D'ANGELO WR (2002) Sources of the scalp-recorded amplitude-modulation following response. J Am Acad Audiol 13(4):188–204

LIBERMAN MC, EPSTEIN MJ, CLEVELAND SS, WANG H, MAISON SF (2016) Toward a differential diagnosis of hidden hearing loss in humans. PLoS One 11(9):1–15

LIBERMAN LD, LIBERMAN MC (2015) Dynamics of cochlear synaptopathy after acoustic overexposure. J Assoc Res Otolaryngol 16:205–219. https://doi.org/10.1007/s10162-015-0510-3

LIN FR, NIPARKO JK, FERRUCCI L (2011) Hearing loss prevalence in the United States. Arch Intern Med 171(20):1851–1852

LOBARINAS E, SALVI R, DING D (2013) Insensitivity of the audiogram to carboplatin induced inner hair cell loss in chinchillas. Hear Res 302:113–120

Long GR, Talmadge CL, Lee J (2008) Measuring distortion product otoacoustic emissions using continuously sweeping primaries. J Acoust Soc Am 124:1613–1626

Makary CA, Shin J, Kujawa SG, Liberman MC, Merchant SN (2011) Age-related primary cochlear neuronal degeneration in human temporal bones. J Assoc Res Otolaryngol 12(6):711–717

Mepani AM, Verhulst S, Liberman MC, Maison S. (2020) Detection of cochlear synaptopathy using EFRs: influence of stimulus envelope. Poster presentation at the American Auditory Society Scientific and Technology Meeting in Scottsdale, AZ

Mills J, Schmiedt R, Schulte B, Dubno J (2006) Age-related hearing loss: a loss of voltage, not hair cells. Semin Hear 27:228–236

Otte J, Schuknecht HF, Kerr AG (1978) Ganglion cell populations in normal and pathological human cochleae: implications for cochlear implantation. Laryngoscope. 88:1231–1246. https://doi.org/10.1288/00005537-197808000-00004

Parthasarathy A, Kujawa SG (2018) Synaptopathy in the aging cochlea: characterizing early-neural deficits in auditory temporal envelope processing. J Neurosci 38(32):7108–7119

Prendergast G, Guest H, Munro KJ, Kluk K, Leger A, Hall DA, Heinz MG, Plack CJ (2017) Effects of noise exposure on young adults with normal audiograms I: electrophysiology. Hear Res 344:68–71

Pujol R, Lenoir M, Robertson D, Eybalin M, Johnstone BM (1985) Kainic acid selectively alters auditory dendrites connected with cochlear inner hair cells. Hear Res 18:145–151

Salvi RJ, Sun W, Ding DL, Chen GD, Lobarinas E, Wang J, Radziwon K, Auerbach BD (2017) Inner hair cell loss disrupts hearing and cochlear function leading to sensory deprivation and enhanced central auditory gain. Front Neurosci 10:1–14. https://doi.org/10.3389/fnins.2016.00621

Schaette R, McAlpine D (2011) Tinnitus with a normal audiogram: physiological evidence for hidden hearing loss and computational model. J Neurosci 31(38):13452–13457

Schermuly L, Klinke R (1985) Change of characteristic frequency of pigeon primary auditory afferents with temperature. J Comp Phys A 156:209–211. https://doi.org/10.1007/BF00610863

Schmiedt, RA. (2010). The physiology of cochlear presbycusis. In: Gordon-Salant S et al. (eds.) The aging auditory system, Springer handbook of auditory research 34, Springer Science + Business Media, pp 9-38

Schoonhoven R, Boden CJ, Verbunt JPA, De Munck JC (2003) A whole head MEG study of the amplitude-modulation-following response: phase coherence, group delay and dipole source analysis. Clin Neurophysiol 114(11):2096–2106

Schrode KM, Muniak MA, Kim YH, Lauer AM (2018) Central compensation in auditory brainstem after damaging noise exposure. eNeuro. 5(4):ENEURO.0250–ENEU18.2018. https://doi.org/10.1523/ENEURO.0250-18.2018

Schuknecht HF, Woellner RC (1953) Hearing losses following partial sectioning of the cochlear nerve. Laryngoscope. 63:441–465

Shaheen LA, Valero MD, Liberman MC (2015) Towards a diagnosis of cochlear neuropathy with envelope following responses. J Assoc Res Otolaryngol 16(6):727–745

Shero M, Salvi RJ, Chen L, Hashino E (1998) Excitotoxic effect of kainic acid on chicken cochlear afferent neurons. Neurosci Lett 257:81–84. https://doi.org/10.1016/S0304-3940(98)00821-0

Sun H, Salvi RJ, Ding DL, Hashino E, Shero M, Zheng XY (2000) Excitotoxic effect of kainic acid on chicken otoacoustic emissions and cochlear potentials. J Acoust Soc Am 107:2136–2142. https://doi.org/10.1121/1.428495

Sun H, Hashino E, Ding DL, Salvi RJ (2001) Reversible and irreversible damage to cochlear afferent neurons by kainic acid excitotoxicity. J Comp Neurol 430:172–181

Valero MD, Burton JA, Hauser SN, Hackett TA, Ramachandran R, Liberman MC (2017) Noise-induced cochlear synaptopathy in rhesus monkeys (*Macaca mulatta*). Hear Res 353:213–223

Verhulst S, Altoe A, Vasilkov V (2018) Computational modeling of the human auditory periphery: auditory-nerve responses, evoked potentials and hearing loss. Hear Res 360:55–75

Wong SJ, Abrams KS, Amburgey KN, Wang Y, Henry KS (2019) Effects of selective auditory-nerve damage on the behavioral audiogram and temporal integration in the budgerigar. Hear Res 374:24–34

Yeend I, Beach EF, Sharma M, Dillon H (2017) The effects of noise exposure and musical training on suprathreshold auditory processing and speech perception in noise. Hear Res 353:224–236

Yuan Y, Shi F, Yin Y, Tong M, Lang H, Polley DB, Liberman MC, Edge ASB (2014) Ouabain-induced cochlear nerve degeneration: synaptic loss and plasticity in a mouse model of auditory neuropathy. J Assoc Res Otolaryngol 15:31–43. https://doi.org/10.1007/s10162-013-0419-7

Zaaroor M, Starr A (1991) Auditory brain-stem evoked potentials in cat after kainic acid induced neuronal loss. I. Superior olivary complex. Electroencephaolgr Clin Neurophysiol 80:422–435. https://doi.org/10.1016/0168-5597(91)90091-b

Zheng XY, Wang J, Salvi RJ, Henderson D (1996) Effects of kainic acid on the cochlear potentials and distortion product otoacoustic emissions in chinchilla. Hear Res 95:161–167. https://doi.org/10.1016/0378-5955(96)00047-0

Zhong Z, Henry KS, Heinz MG (2014) Sensorineural hearing loss amplifies neural coding of envelope information in the central auditory system of chinchillas. Hear Res 309:55–62